Complexes of lanthanides with spin-labeled pyrazolylquinoline

ARTICLE *in* RUSSIAN CHEMICAL BULLETIN · JULY 2015

Impact Factor: 0.48 · DOI: 10.1007/s11172-014-0621-8

Full Articles

Complexes of lanthanides with spin-labeled pyrazolylquinoline*

E. V. Tretyakov,[a]★ S. V. Fokin,[a] E. M. Zueva,[b] A. O. Tkacheva,[a] G. V. Romanenko,[a] A. S. Bogomyakov,[a] S. V. Larionov,[c] S. A. Popov,[d] and V. I. Ovcharenko[a]

[a]*International Tomography Center, Siberian Branch of the Russian Academy of Sciences, 3a ul. Institutskaya, 630090 Novosibirsk, Russian Federation. E-mail: Victor.Ovcharenko@tomo.nsc.ru*
[b]*Department of Inorganic Chemistry, Kazan National Research Technological University, 68 ul. K. Marksa, 420015 Kazan, Russian Federation.*
[c]*A. V. Nikolaev Institute of Inorganic Chemistry, Siberian Branch of the Russian Academy of Sciences, 3 prosp. Akad. Lavrentieva, 630090 Novosibirsk, Russian Federation.*
[d]*N. N. Vorozhtsov Novosibirsk Institute of Organic Chemistry, Siberian Branch of the Russian Academy of Sciences, 9 prosp. Akad. Lavrentieva, 630090 Novosibirsk, Russian Federation.*

The reactions of Eu^{III}, Gd^{III}, and Tb^{III} hexafluoroacetylacetonates with 4,4,5,5-tetramethyl-2-[1-(4-methylquinolin-2-yl)-1*H*-pyrazol-4-yl]-4,5-dihydro-1*H*-imidazole-3-oxide-1-oxyl (L) afford heterospin complexes $[Ln(hfac)_3L_2]$. The X-ray diffraction studies of the complexes showed that the ligand L is coordinated in a monodentate fashion through the oxygen atom of the >N—O group. According to the magnetochemical data, at temperatures below 3 K the complex $[Tb(hfac)_3L_2]$ exhibits properties of a single-molecule magnet with an anisotropy barrier of 12.2 cm^{-1}.

Key words: lanthanides, pyrazolylquinolines, nitroxyl radicals, single-molecule magnets.

Single-molecule magnets[1—3] were discovered in the beginning of the 1990s. Despite very low (below 3—4 K) operating temperatures of these magnets, they attracted great interest, since they offered an opportunity to considerably increase the data density and to design working parts of a quantum computer.[4,5] Therefore, the first communications were followed by a growing number of works with abundant examples of single-molecule magnets (SMM) with various structures.[3] As a result, certain approaches in the field of SMM design have been elaborated, among which was the preparation of SMM based on lanthanide nitroxyl complexes implying the coordination of the paramagnetic >N—O group.[6] Examples of SMM based on mononuclear Tb^{III} and Dy^{III} complexes with one paramagnetic ligand,[7—11] a Tb^{III} complex containing two nitronyl nitroxide radicals in the coordination sphere,[12] binucler Tb^{III} and Dy^{III} complexes,[13—19] and a Dy^{III} poly-

* Dedicated to Academician of the Russian Academy of Sciences O. N. Chupakhin on the occasion of his 80th birthday.

Published in Russian in *Izvestiya Akademii Nauk. Seriya Khimicheskaya,* No. 7, pp. 1459—1464, July, 2014.
1066-5285/14/6307-1459

mer chain complex[20] are known. Among these compounds, of special note are Tb^{III} complexes for which the energies of the barriers for relaxation of the magnetization (U_{eff}) are quite high reaching 20.4 cm^{-1} (the preexponential factor $\tau_0 = 2.99 \cdot 10^{-8}$ s) in $[Tb(hfac)_3(NN\text{-}PhOEt)_2]$ (NN-PhOEt is 4-ethoxyphenyl-substituted nitronyl nitroxide and hfac is hexafluoroacetylacetonate ion) and 20 cm^{-1} ($\tau_0 = 5.9 \cdot 10^{-9}$ s) in $[Tb(hfac)_3(NN\text{-}5\text{-}Br\text{-}3py)]_2$, where NN-5-Br-3py is spin-labeled pyridine.

We found a novel rare-earth metal complex $[Tb(hfac)_3L_2]$, where L is 4,4,5,5-tetramethyl-2-[1-(4-methylquinoline-2-yl)-1*H*-pyrazol-4-yl]-4,5-dihydro-1*H*-imidazole-3-oxide-1-oxyl, which not only shows the behavior of a single-molecule magnet, but also contains the organic luminescent moiety. Note that we have used the ligand L earlier to elucidate the mechanism of luminescence quenching by nitroxyl radicals and found[21] the energy transfer from the photoexcited pyrazolylquinoline moiety to the paramagnetic group, which resulted in emission in the range of 650—850 nm. Taking into account the nature of a rare-earth element (class A metal), we attempted to synthetize a polyfunctional molecule where, on the one hand, the single-molecule magnet moiety would form due to the formation of a three-center exchange cluster upon coordination of the paramagnetic ligand through the >N—O oxygen atom, and, on the other hand, a luminescent label would be present in this molecule.

Results and Discussion

Heterospin complexes $[Ln(hfac)_3L_2]$ (Ln = Eu, Gd, Tb) were prepared in 40—50% yields by the reaction of $[Ln(hfac)_3(H_2O)_2]$ with L.

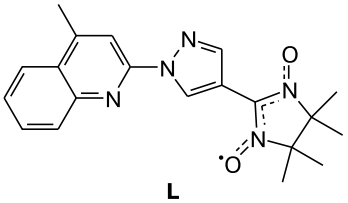

L

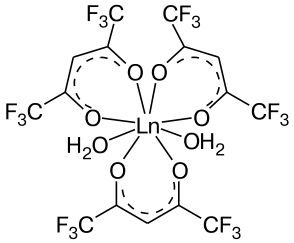

$[Ln(hfac)_3(H_2O)_2]$

According to the X-ray diffraction data, the resulting complexes $[Ln(hfac)_3L_2]$ are isostructural and have molecular structure. The molecular symmetry is C_2 (the two-fold rotation axis passes through the Ln atom and the C(3) atom of one of the hfac ligands (Fig. 1)). The coordination environment of the Ln atom is a square antiprism whose square faces are rotated by an angle of ~30°. The Ln—O bond lengths are in the range of 2.3441(18)—2.401(3) Å, the Gd—O_{NO} and Tb—O_{NO} distances are virtually equal (2.387(2) Å), and the corresponding distance in the Eu^{III} complex is 2.398(2) Å. Note that the N—O bond legnths for the coordinated >N—O group (1.298(3)—1.312(3) Å) are longer than those for the non-coordinated one (1.268(3)—1.270(4) Å).

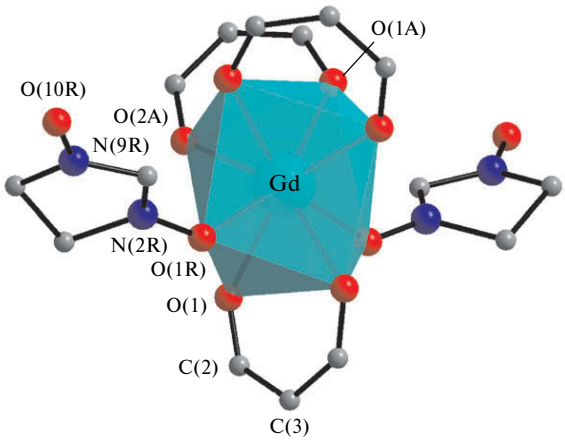

Fig. 1. Molecular structure of $[Gd(hfac)_3L_2]$ (H atoms, CH_3 and CF_3 groups, and bicyclic moieties L are omitted for clarity). *Note.* Figures 1, 2, and 6 are available in full color in the on-line version of the journal (http://www.springerlink.com).

The fragment of the $[Ln(hfac)_3L_2]$ packing is shown in Fig. 2. The molecules in the crystal structure are arranged so that the quinoline rings L of the neighboring complexes are in parallel planes at a distance of ~3.3 Å. The distances between the paramagnetic centers of the neighboring molecules are quite long and exceed 6.0 and 10.4 Å for $O_{NO}\cdots O_{NO}$ and Ln···Ln, respectively.

For $[Gd(hfac)_3L_2]$, μ_{eff} at 300 K is 8.54 μ_B and, with decreasing the temperature, increases slowly to 9.92 μ_B at 5 K (Fig. 3). The high-temperature value of μ_{eff} agrees well with the theoretical value (8.31 μ_B) for three non-interacting paramagnetic centers: one Gd^{3+} ion ($S = 7/2$ at $g = 2$) and two nitroxyl radicals ($S = 1/2$ at $g = 2$). The low-temperature value of μ_{eff} is close to 9.95 μ_B for the paramagnetic center with $S = 9/2$ at $g = 2$, which suggests the ferromagnetic ordering of spins within three-spin clusters {>NO...Gd^{III}...ON<}.

To simulate the $\mu_{eff}(T)$ function for $[Gd(hfac)_3L_2]$, we performed quantum chemical calculations of the intra- and intermolecular isotropic exchange parameters. According to the calculations, the ferromagnetic exhange ($J_{Gd-R^2} = 1.0$ cm^{-1}, $J_{Gd-R^2} = 1.1$ cm^{-1}) predominates in the heterospin cluster of the $[Gd(hfac)_3L_2]$ molecule and the exchange interaction between the nitroxyl groups has

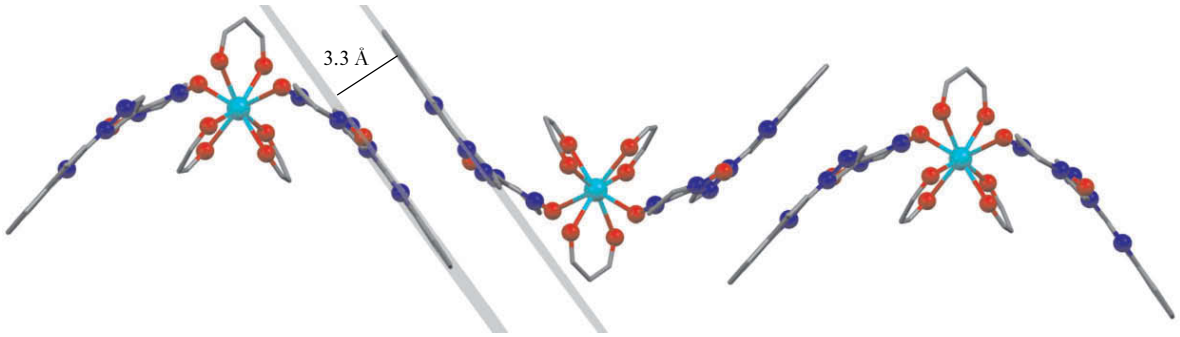

Fig. 2. Mutual arrangement of the $[Ln(hfac)_3L_2]$ molecules in the crystal.

antiferromagnetic nature ($J_{R^1-R^2} = -9.3$ cm^{-1}). The nitroxyl groups of the neighboring molecules are also coupled by an antiferromagnetic interaction; however, its energy is negligibly low ($J_{R-R^*} \approx -0.04$ cm^{-1}). For this reason, let us ignore the effect of intermolecular exchange interactions on the magnetic properties of the $[Gd(hfac)_3L_2]$ complex. Note that quantum chemical calculations slightly underestimate the energy of ferromagnetic exchange between the Gd^{3+} ion and nitroxyls (J_{Gd-R}). Thus, for the calculated values the ground state of the $[Gd(hfac)_3L_2]$ molecule has $S = 7/2$. However, the total spin of its ground exchange multiplet of the $[Gd(hfac)_3L_2]$ molecule is very sensitive to the change in the J_{Gd-R} parameters and, starting from $J_{Gd-R} = 2.7$ cm^{-1} (at a fixed value of $J_{R^1-R^2} = -9.3$ cm^{-1}), the ground state becomes that observed experimentally with $S = 9/2$ (Fig. 3).

The $\mu_{eff}(T)$ function was simulated in terms of the isotropic model in the isolated exchange clusters approximation using the exchange Hamiltonian

$$H = -2J_{Gd-R}[(\vec{S}_{Gd} \cdot \vec{S}_{R^1}) + (\vec{S}_{Gd} \cdot \vec{S}_{R^2})] - \\ - 2J_{R1-R2}(\vec{S}_{R^1} \cdot \vec{S}_{R^2}),$$

assigning $J_{Gd-R} = 2.7$ cm^{-1} and $J_{R^1-R^2} = -9.3$ cm^{-1} as the starting values. The resulted optimum values of the g-factor and exchange parameters J_{Gd-R} and $J_{R^1-R^2}$ are 2.01(±0.01) and 4.8(±0.2) cm^{-1} and −9.5(±0.4) cm^{-1}, respectively.

For $[Eu(hfac)_3L_2]$, μ_{eff} at 300 K is 4.23 μ_B and, with decreasing the temperature, decreases first slowly and, then at the temperature below 30 K, decreases dramatically to 0.53 μ_B at 2 K (Fig. 4). The high-temperature value of μ_{eff} agrees well with the theoretical one (4.27 μ_B) for three non-interacting paramagnetic centers: one Eu^{III} (the typical value $\mu_{eff} \approx 3.5$ μ_B) and two nitroxyls ($S = 1/2$ at $g = 2$).

The ground state of Eu^{III} is singlet ($^7F_0$), but there are closly spaced levels with different J-states, whose population decreases dramatically with a decrease in the temperature. Therefore, in the low-temperature range, the magnetic behavior of $[Eu(hfac)_3L_2]$ will be defined only by the exchange interactions between the nitroxyl spins. Taking into acount the fact that the Eu—O distance is slightly longer than Gd—O, it is possible to ignore the exchange interactions between Eu^{III} and nitroxyls. Indeed, the $\mu_{eff}(T)$ dependence is well described by the equation obtained upon summing up the contributions from the

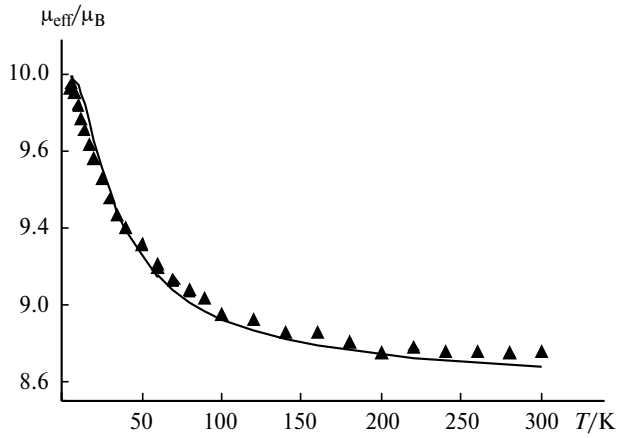

Fig. 3. $\mu_{eff}(T)$ dependence for $[Gd(hfac)_3L_2]$; the experimental values are shown as points and the calculated ones are shown as a curve.

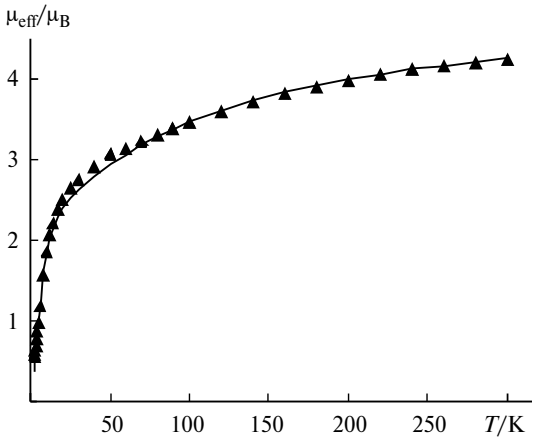

Fig. 4. $\mu_{eff}(T)$ dependence for $[Eu(hfac)_3L_2]$; the experimental values are shown as points and the calculated ones are shown as a curve.

Eu^{3+} ion and exchange-coupled nitroxyls ($H = -2J(\vec{S}_{R1} \cdot \vec{S}_{R2})$) to the magnetic susceptibility[22]:

$$\chi = \chi_{Eu} + \chi_{R-R},$$

where $\chi_{R-R} = \frac{6N\mu_B^2 g^2}{3kT} \frac{1}{3 + e^{-2J/kT}}$,

$$\chi_{Eu} = K \frac{42 + A + B + C + D + E + F}{1 + 3e^{-x} + 5e^{-3x} + 7e^{-6x} + 9e^{-10x} + 11e^{-15x} + 13e^{-21x}},$$

$$K = \frac{N\mu_B^2}{6kTx}, x = \frac{\lambda}{kT},$$

$$A = (27x - 3)e^{-x}, B = (135x - 5)e^{-3x},$$

$$C = (378x - 7)e^{-6x}, D = (810x - 9)e^{-10x},$$

$$E = (1485x - 11)e^{-15x}, F = (2457x - 13)e^{-21x}.$$

At a *g*-factor equal to 2.0 (fixed), the optimum values of the spin-orbital coupling parameter λ and the exchange parameter *J* are 259(±4) and −6.0(±0.2) cm^{-1}, respectively. Thus, the antiferromagnetic interaction between the nitroxyl spins and the decrease in the population of Eu^{III} magnetic levels cause a decrease in μ_{eff} with decreasing the temperature.

For the microcrystalline sample of $[Tb(hfac)_3L_2]$, a decrease in the temperature leads to an increase in μ_{eff} up to 15.25 μ_B at 8 K, which is followed by a sharp decrease in μ_{eff} (Fig. 5, *a*). Such behavior suggests a predominance of the ferromagnetic exchange in the solid phase, which evidently occurs between Tb^{III} and the coordinated nitroxyls.

With increasing the temperature, μ_{eff} decreases to 11.36 μ_B at 300 K. The μ_{eff} value tends to its limit value corresponding to the theoretical value of 10.02 μ_B for three non-interacting paramagnetic centers: one Tb^{III} ($^7F_6$ ground state, $g_J = 3/2$) and two nitroxyl radicals ($S = 1/2$ at $g = 2$).

The dependence of the magnetization of $[Tb(hfac)_3L_2]$ at 2 K on the external magnetic field strength is non-linear and, at ~10 kOe, achieves the saturation being 8.9 $N\mu_B$ (49.7 kG cm^3 mol^{-1}), which is close to the theoretical value of 9 $N\mu_B$ for Tb^{III} (Fig. 5, *b*). The standard measurements in alternate magnetic fields of 100—1500 Hz with a strength of 3 Oe in the temperature range of 2—4.8 K revealed the frequency dependence of the in-phase χ′ and out-of-phase χ″ components of the magnetic susceptibility (Fig. 6). The χ″(*T*) function displays a maximum which shifts to the high-temperature region with increasing the alternate magnetic field frequency, thus allowing assignment of $[Tb(hfac)_3L_2]$ to a family of single-molecule magnets.

The magnetization relaxation rate obtained from the data on magnetic susceptibility in the alternate magnetic field follows the Arrhenius law $\tau = \tau_0 e^{-U_{eff}/kT}$ (τ is the magnetization relaxation time, U_{eff} is the energy barrier for the magnetization relaxation, *k* is the Boltzmann constant, and τ_0 is the preexponential factor). Figure 7 shows the experimental dependence of ln(τ) on $1/T$ and its linear regression by the Arrhenius law. For the complex $[Tb(hfac)_3L_2]$ under study, the optimum values of the parameters U_{eff} and τ_0 are 12.2(±0.6) cm^{-1} and $6 \cdot 10^{-7}$ s, respectively.

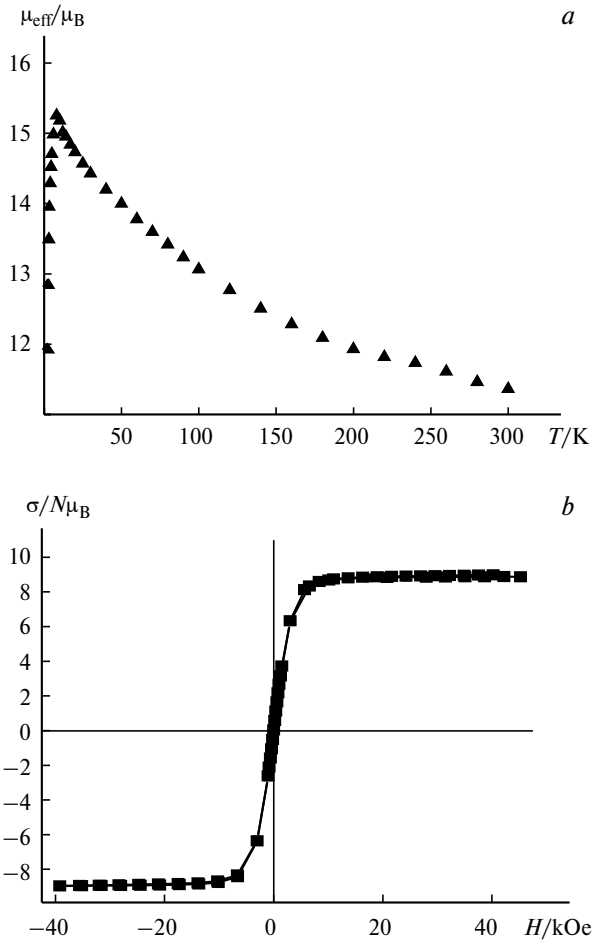

Fig. 5. Experimental $\mu_{eff}(T)$ dependence (*a*) and magnetization as a function of the external magnetic field strength at 2 K (*b*) for $[Tb(hfac)_3L_2]$.

Thus, in the present work the heterospin Eu^{III}, Gd^{III}, and Tb^{III} complexes of the composition $[Ln(hfac)_3L_2]$ containing the hexafluoroacetylacetonate ion and nitroxyl radicals in the coordination sphere were prepared. It was shown that in the $[Gd(hfac)_3L_2]$ complex there occurs the ferromagnetic exchange interaction between the lanthanide ion and each nitroxyl group, the energy of which reaches 4.8 cm^{-1}. The $[Tb(hfac)_3L_2]$ complex demonstrates the behavior typical of a single-molecule magnet with a magnetization relaxation barrier of ~12 cm^{-1} and preexponential factor of $6 \cdot 10^{-7}$ s.

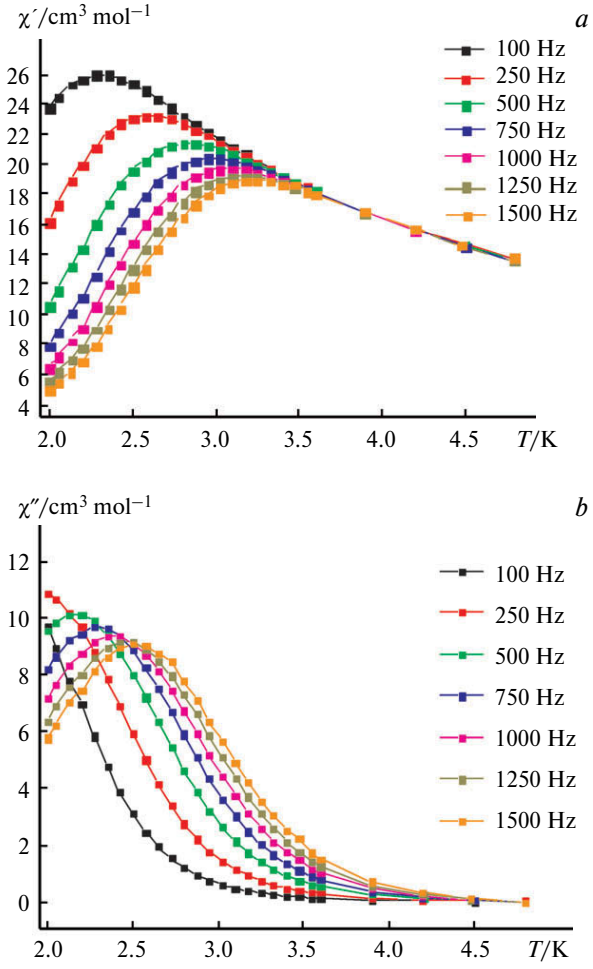

Fig. 6. Temperature dependences of the real χ' (*a*) and imaginary χ'' (*b*) parts of the dynamic magnetic susceptibility for $[Tb(hfac)_3L_2]$ in the absence of constant magnetic field: ν = 100, 250, 500, 750, 1000, 1250, and 1500 Hz.

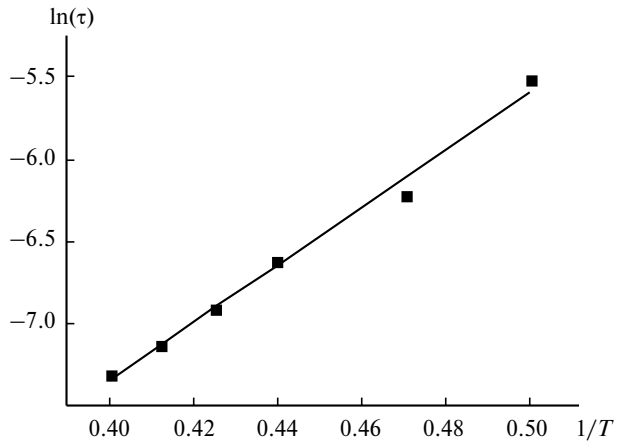

Fig. 7. Linear regression (R = 0.991) of the experimental function ln(τ)—1/T for $[Tb(hfac)_3L_2]$.

Experimental

Elemental analysis was performed on a Euro EA 3000 microanalyzer at the Chemical Service Center of Joint Use of the Siberian Branch of the RAS. Magnetochemical experiments were performed on a Quantum Design MPMSXL SQUID magnetometer in the temperature range of 2—300 K. Commercially available reagents and solvents were used without additional purification. 4,4,5,5-Tetramethyl-2-(1-(4-methylquinolin-2-yl)-1*H*-pyrazol-4-yl)-4,5-dihydro-1*H*-imidazole-3-oxide-1-oxyl[21] and $[Ln(hfac)_3(H_2O)_2]$ (Ln = Eu, Gd, Tb)[23] were synthesized according to the published procedures.

Bis{4,4,5,5-tetramethyl-2-[1-(4-methylquinolin-2-yl)-1*H*-pyrazol-4-yl]-4,5-dihydro-1*H*-imidazole-3-oxide-1-oxyl-*O*}tris-(1,1,1,5,5,5-hexafluoropentane-2,4-dionato-*O*,*O*′)europium, $[Eu(hfac)_3L_2]$. A mixture of 4,4,5,5-tetramethyl-2-[1-(4-methylquinolin-2-yl)-1*H*-pyrazol-4-yl]-4,5-dihydro-1*H*-imidazole-3-oxide-1-oxyl (0.050 g, 0.136 mmol) and $[Eu(hfac)_3(H_2O)_2]$ (0.055 g, 0.068 mmol) was dissolved in benzene (4 mL) with heating to 50 °C, filtered, covered with a layer of *n*-hexane (5 mL), and kept for 20 h at room temperature. The needle-like crystals that formed were filtered off and washed with cold *n*-hexane to yield dark-blue crystals (0.048 g, 47%). Found (%): C, 44.9; H, 3.2; F, 22.1; N, 9.7. $C_{55}H_{47}EuF_{18}N_{10}O_{10}$. Calculated (%): C, 44.0; H, 3.2; F, 22.8; N, 9.3.

Bis{4,4,5,5-tetramethyl-2-[1-(4-methylquinolin-2-yl)-1*H*-pyrazol-4-yl]-4,5-dihydro-1*H*-imidazole-3-oxide-1-oxyl-*O*}tris-(1,1,1,5,5,5-hexafluoropentane-2,4-dionato-*O*,*O*′)gadolinium, $[Gd(hfac)_3L_2]$ was prepared analogously to $[Eu(hfac)_3L_2]$. The yield was 0.046 g (45%), dark-blue crystals. Found (%): C, 44.4; H, 3.0; F, 22.5; N, 9.3. $C_{55}H_{47}F_{18}GdN_{10}O_{10}$. Calculated (%): C, 43.8; H, 3.1; F, 22.7; N, 9.3.

Bis{4,4,5,5-tetramethyl-2-[1-(4-methylquinolin-2-yl)-1*H*-pyrazol-4-yl]-4,5-dihydro-1*H*-imidazole-3-oxide-1-oxyl-*O*}tris-(1,1,1,5,5,5-hexafluoropentane-2,4-dionato-*O*,*O*′)terbium, $[Tb(hfac)_3L_2]$. To a solution of 4,4,5,5-tetramethyl-2-[1-(4-methylquinolin-2-yl)-1*H*-pyrazol-4-yl]-4,5-dihydro-1*H*-imidazole-3-oxide-1-oxyl (0.050 g, 0.136 mmol) in benzene (5 mL) heated to 50 °C, $[Tb(hfac)_3(H_2O)_2]$ (0.111 g, 0.136 mmol) dissolved in benzene (3 mL) and diethyl ether (10 mL) were added. The resulting mixture was filtered and the solution was kept for 96 h at 5 °C. The product formed was filtered off and washed with cold *n*-hexane. The yield was 0.040 g (39%), dark-blue crystals. Found (%): C, 43.0; H, 3.1; F, 22.9; N, 9.0. $C_{55}H_{47}F_{18}N_{10}O_{10}Tb$. Calculated (%): C, 43.8; H, 3.1; F, 22.7; N, 9.3.

X-ray diffraction study. The X-ray diffraction data sets for the single crystals of all compounds were collected on a Smart Apex Duo diffractometer (Cu or Mo radiation, graphite monochromator, T = 240 K, the absorption correction was applied using the SADABS program). The structures were solved by direct methods and refined by the full-matrix least-squares method with anisotropic displacement parameters for all non-hydrogen atoms. Hydrogen atoms were included into the refinement in the geometrically calculated positions and their temperature factors U_H were taken as 1.2-fold higher than those for the thereto bonded carbon and oxygen atoms. All calculations related to the structure solution and refinement were performed using the Bruker Shelxtl (Version 6.14) software package. The crystallographic characteristics of the compounds under study and X-ray data collection and refinement statistics were deposited in the Cambridge Crystallographic Data Centre (CCDC No. 1008762—

1008764; deposit@ccdc.cam.ac.uk; http://www.ccdc.cam.ac.uk/data_request/cif).

The crystalls of all complexes $[Ln(hfac)_3L_2]$ are monoclinic, space group $C2/c$, $Z = 4$.

Complex [Eu(hfac)$_3$L$_2$], $C_{55}H_{47}F_{18}EuN_{10}O_{10}$, $M = 1501.99$, $a = 31.352(3)$ Å, $b = 10.8211(8)$ Å, $c = 20.057(2)$ Å, $\beta = 111.466(6)°$, $V = 6332.6(9)$ Å^3; $d_{calc} = 1.575$ g cm^{-3}, μ(Mo-Kα) = 1.106 mm^{-1}, 27296 reflections were measured ($\theta < 28.02°$), 7573 of which were unique and 3874 reflections were with $I > 2\sigma(I)$, 427 refined parameters, GOOF = 0.815, $R_1 = 0.0444$, and $wR_2 = 0.0737$.

Complex [Gd(hfac)$_3$L$_2$], $C_{55}H_{47}F_{18}GdN_{10}O_{10}$, $M = 1507.28$, $a = 31.311(4)$ Å, $b = 10.8241(15)$ Å, $c = 20.101(3)$ Å, $\beta = 111.680(7)°$, $V = 6330.8(15)$ Å^3; $d_{calc} = 1.581$ g cm^{-3}, μ(Mo-Kα) = 1.163 mm^{-1}, 27691 reflections were measured ($\theta < 28.13°$), 7660 of which were unique and 5627 reflections were with $I > 2\sigma(I)$, 481 refined parameters, GOOF =1.142, $R_1 = 0.0430$, and $wR_2 = 0.0930$.

Complex [Tb(hfac)$_3$L$_2$], $C_{55}H_{47}F_{18}TbN_{10}O_{10}$, $M = 1508.94$, $a = 31.224(3)$ Å, $b = 10.8330(11)$ Å, $c = 20.042(2)$ Å, $\beta = 111.585(5)°$, $V = 6304.0(11)$ Å^3; $d_{calc} = 1.590$ g cm^{-3}, μ(Cu-Kα) = 6.562 mm^{-1}, 23229 reflections were measured ($\theta < 60.00°$), 4560 of which were unique and 4227 reflections were with $I > 2\sigma(I)$, 481 refined parameters, GOOF = 1.047, $R_1 = 0.0280$, and $wR_2 = 0.0732$.

Quantum chemical calculations. The calculations of isotropic exchange parameters for the $[Gd(hfac)_3L_2]$ complex were performed by the broken symmetry method using the spin-projected schemes of Noodleman *et al.*[24—27] and Yamaguchi *et al.*[28,29] using the ORCA (version 2.8) program package.[30] Single-determinant wavefunctions (HS and all possible BS determinants) were calculated for the crystallographic structure by the B3LYP/TZVP-DKH method (the calculated values of exchange parameters are given in the text). The TPSSh/TZVP-DKH method gives the close values: $J_{Gd-R^1} = 1.4$ cm^{-1}, $J_{Gd-R^2} = 1.6$ cm^{-1}, and $J_{R^1-R^2} = -13.6$ cm^{-1} (for the intramolecular exchange interactions) and $J_{R-R^*} = -0.07$ cm^{-1} (for the intermolecular exchange). In all cases, the deviation between the calculated and expected values of $\langle\vec{S}^2\rangle_{HS}$ and $\langle\vec{S}^2\rangle_{BS}$ are not more than 0.08. Both spin-projected schemes afford identical values of exchange parameters (to one decimal place).

This work was financially supported by the Russian Foundation for Basic Research (Project Nos 12-03-00067, 13-03-12401, and 14-03-20011), the Council for Grants at the President of the Russian Federation (Program for State Support of Leading Scientific Schools and Young Scientists of the Russian Federation, Grant MK-247.2014.3), the Presidium of the Russian Academy of Sciences (Program No. 44, Project No. 83), and the Siberian Branch of the Russian Academy of Sciences.

References

1. R. Sessoli, L. Hui, A. R. Schake, S. Wang, J. B. Vincent, K. Folting, D. Gatteschi, G. Christou, *J. Am. Chem. Soc.*, 1993, **115**, 1804.
2. R. Sessoli, D. Gatteschi, A. Caneschi, M. A. Novak, *Nature*, 1993, **365**, 141.
3. D. Gatteschi, R. Sessoli, J. Villain, *Molecular Nanomagnets*, Oxford University Press, Oxford, 2006.
4. M. N. Leuenberger, D. Loss, *Nature*, 2001, **410**, 789.
5. A. Ardavan, O. Rival, J. J. L. Morton, S. J. Blundell, A. M. Tyryshkin, G. A. Timco, R. E. P. Winpenny, *Phys. Rev. Lett*,. 2007, **98**, 057201.
6. D. N. Woodruff, R. E. Winpenny, R. A. Layfield, *Chem. Rev.*, 2013, **113**, 5110.
7. P. Hu, M. Zhu, X. Mei, H. Tian, Y. Ma, L. Li, D. Liao, *Dalton Trans.*, 2012, **41**, 14651.
8. X.-L. Wang, L.-C. Li, D.-Z. Liao, *Inorg. Chem.*, 2010, **49**, 4735.
9. E. Coronado, C. Gimenez-Saiz, A. Recuenco, A. Tarazon, F. M. Romero, A. Camon, F. Luis, *Inorg. Chem.*, 2011, **50**, 7370.
10. P. Hu, M. Zhu, X. Mei, H. Tian, Y. Ma, L. Li, D. Liao, *Dalton Trans.*, 2012, **41**, 14651.
11. X.-L. Mei, Y. Ma, L.-C. Li, D.-Z. Liao, *Dalton Trans.*, 2012, **41**, 505.
12. N. Zhou, Y. Ma, C. Wang, G. F. Xu, J.-K. Tang, J.-X. Xu, S.-P. Yan, P. Cheng, L.-C. Li, D.-Z. Liao, *Dalton Trans.*, 2009, **40**, 8489.
13. G. Poneti, K. Bernot, L. Bogani, A. Caneschi, R. Sessoli, W. Wernsdorfer, D. Gatteschi, *Chem. Commun.*, 2007, **18**, 1807.
14. H. Tian, R. Liu, X. Wang, P. Yang, Z. Li, L. Li, D. Liao, *Eur. J. Inorg. Chem.*, 2009, **29—30**, 4498.
15. J.-X. Xu, Y. Ma, D.-Z. Liao, G.-F. Xu, J. Tang, C. Wang, N. Zhou, S.-P. Yan, P. Cheng, L.-C. Li, *Inorg. Chem.*, 2009, **48**, 8890.
16. K. Bernot, F. Pointillart, P. Rosa, M. Etienne, R. Sessoli, D. Gatteschi, *Chem. Commun.*, 2010, **46**, 6458.
17. X.-L. Mei, R.-N. Liu,.C. Wang, P.-P. Yang, L.-C. Li, D.-Z. Liao, *Dalton Trans.*, 2012, **41**, 2904.
18. R. Liu, C. Zhang, L. Li, D. Liao, J.-P. Sutter, *Dalton Trans.*, 2012, **41**, 12139.
19. F. Pointillart, K. Bernot, G. Poneti, R. Sessoli, *Inorg. Chem.*, 2012, **51**, 12218.
20. R. Liu, L. Li, X. Wang, P. Yang, C. Wang, D. Liao, J.-P. Sutter, *Chem. Commun.*, 2010, **46**, 2566.
21. E. V. Tretyakov, V. F. Plyusnin, A. O. Suvorova, S. V. Larionov, S. A. Popov, O. V. Antonova, E. M. Zueva, D. V. Stass, A. S. Bogomyakov, G. V. Romanenko, V. I. Ovcharenko, *J. Lumin.*, 2014, **148**, 33.
22. M. Andruh, E. Bakalbassis, O. Kahn, J. C. Trombe, P. Porchers, *Inorg. Chem.*, 1993, **32**, 1616.
23. K. Miyata, T. Nakagawa, R. Kawakami, Y. Kita, K. Sugimoto, T. Nakashima, T. Harada, T. Kawai, Y. Hasegawa, *Chem. Eur. J.*, 2011, **17**, 521.
24. L. Noodleman, J. G. Norman, Jr., *J. Chem. Phys.*, 1979, **70**, 4903.
25. L. Noodleman, *J. Chem. Phys.*, 1981, **74**, 5737.
26. L. Noodleman, E. R. Davidson, *Chem. Phys.*, 1986, **109**, 131.
27. L. Noodleman, D. A. Case, *Adv. Inorg. Chem.*, 1992, **38**, 423.
28. T. Soda, Y. Kitagawa, T. Onishi, Y. Takano, Y. Shigeta, H. Nagao, Y. Yoshioka, K. Yamaguchi, *Chem. Phys. Lett.*, 2000, **319**, 223.
29. M. Shoji, K. Koizumi, Y. Kitagawa, T. Kawakami, S. Yamanaka, M. Okumura, K. Yamaguchi, *Chem. Phys. Lett.*, 2006, **432**, 343.
30. *Neese F. ORCA — an ab initio, Density Functional and Semiempirical Program Package*, Version 2.8, University of Bonn, Bonn, Germany, 2011.

Received June 9, 2014;
in revised form June 25, 2014